Bioorganic Chemistry 54 (2014) 73–80

Contents lists available at ScienceDirect

Bioorganic Chemistry

journal homepage: www.elsevier.com/locate/bioorg

Synthesis, characterization and ROS-mediated cytotoxic action of novel (*S*,*S*)-1,3-propanediamine-*N*,*N*′-di-2-(3-cyclohexyl)propanoic acid and corresponding esters

Aleksandar Savić [a,1], Sonja Misirlić-Denčić [b,1], Marija Dulović [b], Ljiljana E. Mihajlović-Lalić [a], Maja Jovanović [b], Sanja Grgurić-Šipka [a,*], Ivanka Marković [b,*], Tibor J. Sabo [a]

[a] Faculty of Chemistry, University of Belgrade, Studentski trg 12-16, 11000 Belgrade, Serbia
[b] Institute of Medical and Clinical Biochemistry, Faculty of Medicine, University of Belgrade, Belgrade, Serbia

ARTICLE INFO

Article history:
Received 31 January 2014
Available online 26 April 2014

Keywords:
Amine ligands
Apoptosis
n-Butyl ester
Cyclohexyl analogues
Cytotoxic activity
Oxidative stress

ABSTRACT

This study involves the synthesis and characterization of novel cyclohexyl 1,3-propanediamine-*N*,*N*′-diacetate molecules as well as investigation of their cytotoxic action. New acid **1a** was synthesized by reaction between (*S*)-2-amino-3-cyclohexylpropanoic acid and 1,3-dibromopropane, while the esters (**1b**–**1e**) derived from this acid were obtained by reaction of the corresponding absolute alcohol, thionyl chloride and synthesized acid. All compounds were characterized by IR, ESI-MS, (^{1}H, ^{13}C and HSQC) NMR spectroscopy and elemental analysis. The cytotoxic activity of all compounds was tested on several tumour cell lines: human (U251) and rat (C6) glioma, human promyelocytic leukaemia (HL-60), human neuroblastoma (SHSY-5Y) and mouse fibrosarcoma (L929) as well as primary rat astrocytes. The present study reveals potent antitumour activity of novel purely organic compounds (**1a**–**1e**), which was most pronounced in human glioma (U251) cells. The esterification is required for the novel compounds' cytotoxic action since the *n*-butyl ester **1e** was the most efficient compound. Importantly, *n*-butyl ester **1e** was more toxic to glioma cells in comparison to rat astrocytes, with 24-h IC_{50} values lower than those for cisplatin. *n*-Butyl ester **1e** induced production of reactive oxygen species (ROS) and caused an oxidative-stress-derived accumulation of glioma cells in the G_0/G_1 phase of the cell cycle, as well as caspase activation and DNA fragmentation, suggesting that apoptosis induction plays an important role in the novel compounds' antiglioma action.

1. Introduction

Medicinal chemistry is a rapidly growing field, particularly in the field of drug design and development [1–3]. Generally, metal-based antitumour agents are active due to their metal centre, which is positively charged and thus binds to the negatively charged residues of proteins and nucleic acids and in this manner kills cancer cells [4]. Over the past 40 years, the metal-based antitumour drug cisplatin has, despite numerous side effects [5], been used in treatment of various cancers [6,7]. However, many ruthenium-based drugs are now promising antitumour agents, showing lower toxicity *in vitro* and high activity in *in vivo* models [8]. Some of these agents, e.g. KP1019 and NAMI-A, have even been used in clinical trials with promising results [9,10]. Most of the metal complexes, including the platinum-based compound cisplatin as a typical representative, kill cells by inducing DNA damage followed by oxidative stress, mitochondrial dysfunction and caspase-dependent apoptosis [11]. Unfortunately, the use of cisplatin is restricted because of severe dose-limiting side effects due to the uptake of the drug into all rapidly dividing cells and the body's attempt to excrete the drug through the kidneys. Additionally, the severe side effects of cisplatin result in reduction of dosage, making the dose delivered to tumour cells sub-lethal, particulary to ovarian cancers, which can lead to development of drug resistance [5]. For that reason, organic compounds that lack metal and have an incorporated ethylenediamine group, which is known for its positive contribution to the cytotoxicity effect [12], deserve special attention. Compounds of ethanediamine-*N*,*N*′-diacetate (edda)-type and their derivatives exhibit a structure–activity relationship that has been confirmed through numerous *in vitro* tests

* Corresponding authors. Address: Pasterova 2, 11000 Belgrade, Serbia. Fax: +381 112184330 (S. Grgurić-Šipka). Fax: +381 11 3643 248 (I. Markovic).
E-mail addresses: sanjag@chem.bg.ac.rs (S. Grgurić-Šipka), ivanka@med.bg.ac.rs (I. Marković).
[1] These authors contributed equally to this work.

http://dx.doi.org/10.1016/j.bioorg.2014.04.006
0045-2068/

against various tumour cell lines [13,14]. In the last decade, many compounds of similar structure have been synthesized. There are several reported studies on the cytotoxicity of these substances [15–18]. Among them, esters of (*S*,*S*)-ethanediamine-*N*,*N*′-di-2-(3-cyclohexyl)propanoic acid showed particularly good anticancer activity [18]. The antileukaemic action of these compounds is via caspase-independent apoptosis, associated with oxidative stress, mitochondrial dysfunction and AIF translocation to leukaemic cells' nuclei. In addition, leukaemic patients' peripheral blood mononuclear cells were more sensitive to the cytotoxic action of these compounds than corresponding cells of healthy volunteers [19]. Taking into account all of the above, we decided to synthesize molecules with a similar structure and to explore if elongation of the alkyl chain between the nitrogen atoms by one methylene group could improve the anticancer activity.

In this paper, we report the preparation, characterization and *in vitro* antitumour potential of (*S*,*S*)-1,3-propanediamine-*N*,*N*′-di-2-(3-cyclohexyl)propanoic acid and corresponding methyl, ethyl, *n*-propyl and *n*-butyl esters. The cytotoxic potential of the newly synthesized compounds was determined by MTT assay and was further investigated by flow cytometric analysis of reactive oxygen species (ROS) production, cell cycle distribution and DNA fragmentation.

DNA chirality is considered to be involved in a series of important life events. Investigations demonstrated chiral selectivity of chiral compounds towards DNA [20]. Interactions of newly prepared compounds containing stereocentres will be explored in future work.

2. Results and discussion

2.1. Chemistry

2.1.1. Synthesis of **1a**

(*S*,*S*)-1,3-propanediamine-*N*,*N*′-di-2-(3-cyclohexyl)propanoic acid (Scheme 1) was obtained by the reaction of (*S*)-2-amino-3-cyclohexylpropanoic acid with 1,3-dibromopropane under reflux in water. After addition of diluted hydrochloric acid, a product in hydrochloride form was obtained, and the synthesized compound was soluble in trifluoroacetic acid (TFA) and formic acid [21].

2.1.2. Synthesis of **1b**–**1e**

Methyl, ethyl, *n*-propyl and *n*-butyl esters of (*S*,*S*)-1,3-propanediamine-*N*,*N*′-di-2-(3-cyclohexyl)propanoic acid (Scheme 1) were obtained by the reaction of the acid, corresponding alcohol and thionyl chloride [21]. These esters are soluble in ethanol, formic acid, TFA and partially soluble in water and dimethylsulphoxide (DMSO).

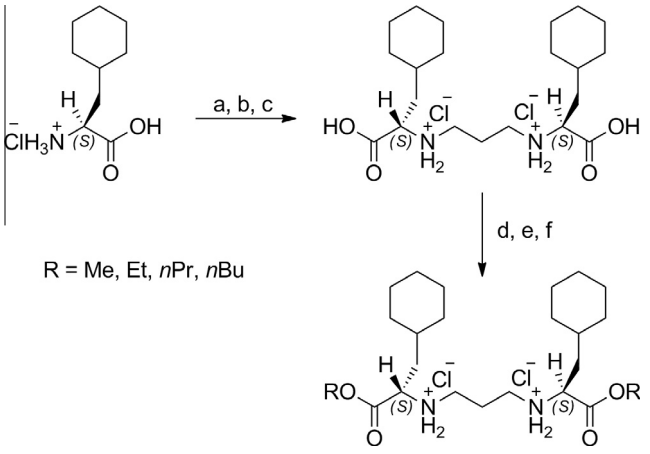

Scheme 1. Reagents and conditions: (a) NaOH/H_2O, 0 °C; (b) 1,3-dibromopropane, reflux, 24 h; (c) NaOH/HCl/EtOH; (d) ROH, $SOCl_2$, 1 h, 0 °C; (e) reflux, 24 h; and (f) acetone, 4 °C.

2.1.3. Spectroscopic studies

In the IR spectra, characteristic absorption bands for carboxylic acid and aliphatic esters were found. Stretching bands for C=O were located in the region 1732–1743 cm^{-1}. Characteristic absorption bands for salts of secondary amines were found in the region 2800–2250 cm^{-1}, while deformation bands for NH_2 were detected around 1550 cm^{-1}. Typical symmetric and asymmetric CH stretching vibrations, which correspond to aliphatic groups, were located in the range 2932 and 2852 cm^{-1} in the form of two bands.

In the ^{1}H NMR spectra of **1a**–**1e**, the signals attributable to cyclohexyl protons were found in the range 0.96–1.98 ppm. Also in this region, protons of the alkyl ester group (**R**CH_2O—) and the NH protons were detected. The obvious triplet located around 2.0 ppm was related to —C**H$_2$**Cy protons. The shift assignable to —NH_2CH_2C**H$_2$**CH_2NH_2— protons were observed around 2.7 ppm, while adjacent protons —NH_2**C H$_2$**CH_2C**H$_2$**NH_2— were found in region 3.43–3.68 in the form of two separated multiplets. A characteristic triplet around 4.30 ppm was assigned to two protons from the —OOCC**H**— moiety. ^{1}H NMR spectra gave clear signals of RC**H$_2$**-O— protons in the range 3.95–4.49 ppm as two separated multiplets. In the ^{1}H NMR spectra of **1a**–**1e** (recorded in TFA), protons of hydrochloride and protons bound to a carboxyl group (**1a**) could not be detected because of the fast exchange of these protons with solvent protons. In the ^{1}H NMR spectra of these compounds (recorded in DMSO), these protons were detected at 9.44 ppm for **1a** and 9.61 and 10.04 ppm for **1b**. Based on HSQC NMR spectra, the correlation of C—H was determined for all compounds. In the ^{13}C NMR spectra, all signals were detected at the expected chemical shifts. Cyclohexyl carbons were found in the range 27.40–36.41 ppm. Carbons from the diamine moiety were located around 25.80 ppm (—NH_2CH_2**C**$H_2CH_2NH_2$—) and 47.20 ppm (—NH_2**C**H_2 CH_2**C**H_2NH_2—). Typical shifts for the carbonyl group of acid **1a** were detected at 175.45 ppm, whereas the signal of this group of **1b**–**1e** appeared at a slightly lower chemical shift (172.77–173.22 ppm). The mass spectra of all compounds contained the peaks of $[M-2HCl+H]^+$ and $[M-2HCl+2H]^{2+}$ ions, which matched the calculated molecular mass.

2.2. Biology

2.2.1. In vitro cytotoxic action of novel compounds

We assessed the antitumour potential of the five novel metal-free compounds of purely organic nature (**1a**–**1e**) in five tumour cell lines: rat and human glioma (C6 and U251, respectively), mouse fibrosarcoma (L929), human neuroblastoma (SHSY-5Y) and human promyelocytic leukaemia (HL-60), as well as in culture of primary rat astrocytes. The calculated IC_{50} values after 24-h exposure to each compound are presented in Table 1.

The obtained results show lower IC_{50} values for esters compared to the parental acid **1a** in all but one cell line (SH-SY5Y), suggesting that esterification is essential for cytotoxic action. A direct correlation between the cytotoxic potency and the alkyl side-chain length of the investigated compounds was observed because *n*-butyl ester **1e** was the most cytotoxic to all the investigated cell cultures, except for the HL-60 cell line where ethyl ester **1c** and *n*-butyl ester **1e** showed comparable cytotoxic activity (Table 1). Furthermore, IC_{50} values for *n*-butyl ester **1e** were lower than those obtained for the prototypical anticancer drug cisplatin (Table 1). These results indicate that the increase in alkyl side-chain length, together with elongation of the alkyl chain between the nitrogen atoms by one methylene group, contributed to the efficiency of the tested compounds. Cyclohexyl analogues of ethanediaminedipropanoic acid had potent antileukaemic action, but we found no direct correlation between the cytotoxic potency and the alkyl side-chain length of the compounds, since the increase in alkyl side-chain length was associated with the loss of activity of *n*-butyl

Table 1
In vitro cytotoxicity of organic compounds (**1a**–**1e**) determined by MTT assay after 24-h incubation.

Cell line	IC_{50} (μM); 24 h; MTT					
Compound	U251	SH-SY5Y	C6	L929	HL-60	Astrocytes
1a	56.39 ± 11.03	17.48 ± 1.45	42.00 ± 11.91	32.16 ± 8.23	63.2 ± 9.06	n.c.
1b	35.69 ± 0.79	37.54 ± 8.29	54.78 ± 1.26	40.01 ± 4.85	20.4 ± 3.33	42.10 ± 5.14
1c	16.93 ± 0.23	14.18 ± 0.94	15.36 ± 0.91	14.57 ± 0.31	10.9 ± 1.05	12.86 ± 2.93
1d	5.87 ± 0.31	11.54 ± 3.20	7.88 ± 0.26	6.86 ± 1.13	30.2 ± 4.78	18.30 ± 2.42
1e	3.78 ± 0.23 [*,#]	14.41 ± 0.76	5.81 ± 1.56 [*,#]	9.79 ± 0.68	13.1 ± 0.92	16.90 ± 2.65 [#]
Cisplatin	11.5 ± 3.3	n.a.	10.9 ± 3.1	11.2 ± 3.4	17.5 ± 2.4	>100

Values represent the mean ± SD from two independent experiments; (n.a. – not assessed; n.c. – not calculated due to the toxicity of formic acid towards primary astrocytes cell culture.
[*] $p < 0.05$ denotes lower IC_{50} value compared to obtained for astrocytes.
[#] $p < 0.05$ refers to treatment with cisplatin).

ester [19]. On the other hand, the introduction of an additional methylene group between the nitrogen atoms improved the cytotoxicity of (*S*,*S*)-1,3-propanediamine-*N*,*N*′-di-2-(3-cyclohexyl) propanoic acid in comparison with (*S*,*S*)-ethanediamine-*N*,*N*′-di-2-(3-cyclohexyl)propanoic acid, which was not toxic to the HL-60 cell line [19] confirming the validity of the synthetic approach. Nevertheless, ethyl esters of both acids showed comparable cytotoxic action against the HL-60 cell line, indicating that the cytotoxic effect may be tumour-cell-specific. However, *n*-butyl ester **1e** showed superior cytotoxic action in both investigated glioma U251 and C6 cell lines with IC_{50} values significantly lower (four- and three-fold, respectively) in comparison with the primary rat astrocytes. It is noteworthy that the IC_{50} value for *n*-butyl ester **1e** was even lower than the prototypical anticancer drug cisplatin against both investigated glioma cell lines ($p < 0.05$).

n-Butyl ester **1e** (highest antitumour efficiency) and U251 cells (highest sensitivity to cytotoxic action of **1e**) were chosen for further investigation.

2.2.2. Oxidative stress induction by novel organic compounds

Induction of oxidative stress by increased superoxide production, accompanied by mitochondrial membrane depolarization, was recently reported to be responsible for the antileukaemic action of cyclohexyl functionalized ethanediaminediacetate-type ligands [19]. Since the compounds of interest in this study (**1a**–**1e**) have a similar structure as those previously synthesized [19], we explored whether their cytotoxicity is also due to oxidative stress induction. In accordance with the cytotoxicity data, staining with the redox-sensitive fluorochrome dihydrorhodamine (DHR) revealed both time- and dose-dependent increases in ROS production in U251 cells treated with *n*-butyl ester **1e** ($p < 0.01$), with maximum ROS production after 6-h treatment with 6 μM *n*-butyl ester **1e** (Fig. 1A and B). At the same time, production of the superoxide anion increased in a concentration-dependent manner reaching its maximum after 4 h (6 μM) and confirming its role in oxidative stress induction in U251 cells (Fig. 1C). In contrast to the results obtained in human glioma cells, *n*-butyl ester **1e** failed to induce superoxide overproduction in rat astrocytes (Fig. 2B). The oxidative-stress-mediated *n*-butyl ester **1e** antiglioma action might explain its approximately four-fold lower IC_{50} value in U251 glioma cells in comparison with astrocytes.

2.2.3. Novel compounds cause DNA fragmentation, caspase activation and slow down cell cycle progression in U251 cells

We next investigated the mode of cell death (apoptotic or necrotic) and the presence of autophagy in *n*-butyl ester **1e**-treated U251 glioma cells. Apoptosis is characterized by phosphatidylserine exposure on the outer side of the phospholipid bilayer of the cell membrane, chromatin condensation and internucleosomal DNA fragmentation in the absence of plasma membrane damage [22]. In contrast, necrosis is distinguished by plasma membrane breakdown as indicated by release of lactate dehydrogenase (LDH) from the cells. In our experiments, flow cytometric analysis of cell cycle changes in U251 glioma cells, induced by 16- and 24-h treatment with *n*-butyl ester **1e,** revealed a significant increase in the percentage of U251 cells with DNA fragmentation compared to untreated U251 cells ($p < 0.01$) (Fig. 1D and E), which was also time-dependent (10.01% and 26.25% for 16- and 24-h treatment with 6 μM, respectively).

The increase in the percentage of cells with hypodiploid DNA content after treatment with *n*-butyl ester **1e** (24 h; 3 and 6 μM) was associated with accumulation of cells in the G_0/G_1 phase of the cell cycle (Fig. 1E). Since both extrinsic and intrinsic pathways of apoptosis can include activation of caspases, i.e. apoptosis-executing cysteine proteases [21], we next investigated caspase activation in *n*-butyl ester **1e**-treated U251 glioma cells. Treatment with *n*-butyl ester **1e** (6 μM) caused a significant, time-dependent increase in caspase activation in U251 cells (Fig. 1F), which is indicative of apoptosis induction, although neither 16- nor 24-h treatment of U251 glioma cells caused an increase in phosphatidylserine externalization (Fig. 1G). However, a significant increase in phosphatidylserine externalization following the treatment with *n*-butyl ester **1e** was observed in the HL-60 cell line (41.7 ± 3.8% of annexin$^+$ cells), indicating a tumour-cell-specific action of *n*-butyl ester **1e**. In addition, results of the LDH release assay confirmed the lack of U251 cell membrane damage, since 24-h treatment with *n*-butyl ester **1e** (1.5, 3 and 6 μM) failed to induce marked LDH release (99.36%, 98.65% and 97.20% viable cells, respectively) confirming that necrosis is not relevant for *n*-butyl ester **1e** antiglioma action. The apoptosis induction seemed to be fairly selective for glioma cells, since treatment with *n*-butyl ester **1e** (12.5 and 25 μM) failed to induce phosphatidylserine externalization (Fig. 2C) and caspase activation (data not shown) in astrocytes.

These results indicate that *n*-butyl ester **1e** antiglioma action is mediated by induction of apoptosis, as shown by caspase activation and DNA fragmentation.

It has been shown that increased production of ROS can induce autophagy, a process of self-digestion of intracellular components in acidified vesicles called autophagolysosomes [23]. Autophagy can play a pro-survival role in cells under stress conditions, but if extensive, activated inappropriately or in cells that are unable to die by apoptosis, it can be a type of cell death [24]. Our results show that autophagy induction was not observed following treatment with *n*-butyl ester **1e** (1.5, 3 and 6 μM) as no increase in the lysosome-derived cytoplasm acidic content in U251 cells was observed after 24-h treatment (Fig. 1H). Since recent data suggest that autophagy could have a protective role in cisplatin-triggered apoptosis [25], the lack of autophagy induction after treatment with *n*-butyl ester **1e** might contribute to its cytotoxic action.

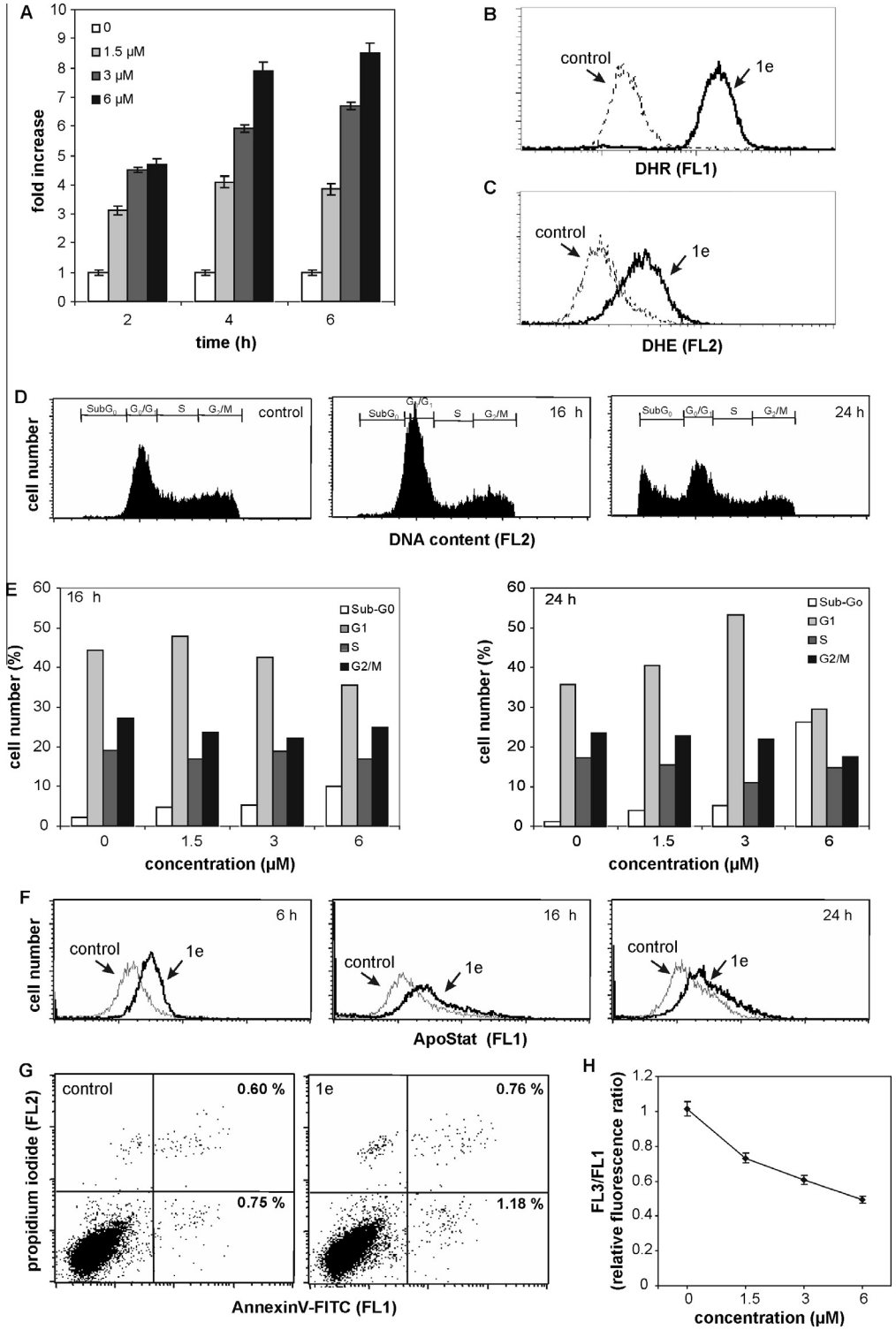

Fig. 1. *n*-Butyl ester **1e** induces oxidative stress, cell cycle arrest, DNA fragmentation and caspase activation in U251 glioma cells but does not induce cytoplasm acidification. (A) Time- and dose-dependent increase in DHR-derived mean fluorescence intensity (FL1) ($p < 0.01$ in comparison with control for each time and dose combination). (B) Maximum DHR fluorescence after 6-h treatment with 6 μM *n*-butyl ester. (C) Superoxide anion FL2 (DHE) mean fluorescence intensity reached its maximum after 4 h (6 μM) of treatment with *n*-butyl ester **1e**. (D) Representative histograms of DNA content in PI-stained U251 cells (control and treatment with 6 μM of *n*-butyl ester **1e**). (E) Representative bar-chart of 16- and 24-h cell cycle analysis of U251 cells treated with *n*-butyl ester **1e** (1.5, 3 and 6 μM) showing G_1-S cell cycle arrest and an increase ($p<0.05$) in the number of cells with hypodiploid DNA content (sub-G_0) in comparison with untreated control. (F) Time-dependent increase in caspase activation, shown by FL1 mean fluorescence intensity in U251 cells treated with *n*-butyl ester **1e** (6 μM). (G) Representative dot-plots of Ann/PI-stained U251 cells showing no increase in the number of Ann^+ cells in *n*-butyl-ester-treated (24 h; 6 μM) U251 cells compared to untreated control. (H) Dose-dependent FL3/FL1 fluorescence ratio decrease confirming lack of U251 cytoplasm acidification after treatment with *n*-butyl **1e** ester. The data in (A) and (H) are mean ± SD values from two independent experiments.

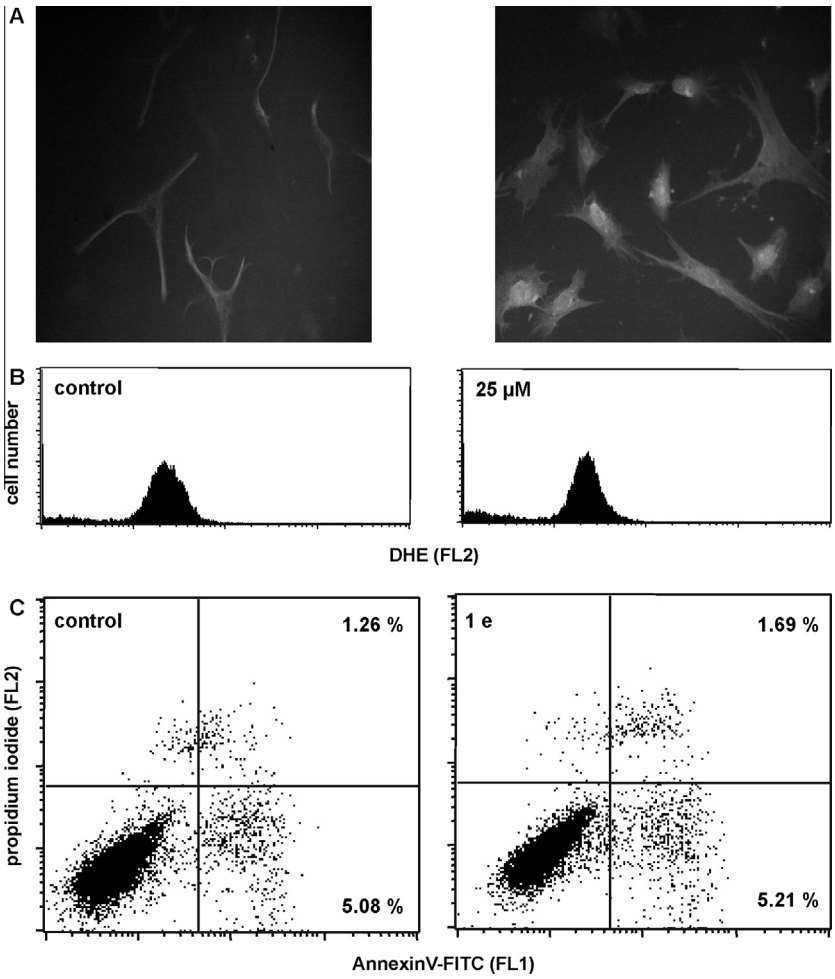

Fig. 2. *n*-Butyl ester **1e** fails to induce superoxide hyperproduction and posphatidylserine externalization in primary Wistar rat astrocytes. (A) Rat astrocyte primary culture verification after immunostaining with rabbit anti-rat (1:400) and FITC-conjugated anti-rabbit (1:1000) antibody: 8-day-old (left) and 21-day-old (right) cultures; magnification 10×. (B) DHE mean fluorescence intensity (FL2) resulting from superoxide anions showed no increase after 2-h treatment with *n*-butyl ester **1e** (25 μM). (C) Representative dot-plots of Ann/PI-stained rat astrocytes showing no increase in the number of Ann^+ cells in *n*-butyl ester **1e**-treated (24 h; 25 μM) rat astrocytes compared to untreated control.

3. Conclusion

In summary, the present work demonstrates the synthesis and characterization of new compounds derived from (*S*)-2-amino-3-cyclohexylpropanoic acid, followed by *in vitro* assessment of anticancer activity in five tumour cell lines: human (U251) and rat (C6) glioma, human promyelocytic leukaemia (HL-60), human neuroblastoma (SH-SY5Y) and mouse fibrosarcoma (L929) as well as primary rat astrocyte cell culture. The results show good antitumour activity of the novel compounds (**1a**–**1e**), which was most pronounced in the human glioma cell line. *n*-Butyl ester **1e** had the most effective cytotoxic action, suggesting that esterification and alkyl-side-chain length are important for antitumour action. Importantly, the *n*-butyl ester **1e** showed good selectivity, as its cytotoxicity towards glioma cells was superior than that towards astrocytes, with IC_{50} values for the U251 cell line that were lower than those for cisplatin. *n*-Butyl ester **1e** induced ROS production in glioma cells, leading to accumulation of cells in the G_0/G_1 phase of the cell cycle, followed by caspase activation and DNA fragmentation. By providing insight into the cytotoxic effects of these novel compounds, these data could contribute to further research of their biological effects alone or as part of different metal complexes.

4. Experimental

4.1. Chemistry

(*S*)-2-amino-3-cyclohexyl-propanoic acid hydrochloride was purchased from Senn Chemicals (Dielsdorf, Switzerland). (*S*,*S*)-1,3-propanediamine-*N*,*N*′-di-2-(3-cyclohexyl)propanoic acid dihydrochloride and corresponding esters were obtained as described in this paper. Solvents were obtained commercially and used without further purification. Elemental analysis was carried out with an Elemental Vario EL III microanalyser. Infrared spectra were recorded on a Nicolet 6700 FT-IR spectrometer using the ATR technique. The NMR spectra were recorded on a Varian Gemini 200 or Bruker Avance III 500 spectrometer. Chemical shifts for ^1H and ^{13}C spectra were referenced to residual ^1H and ^{13}C present in deuterated TFA and DMSO. The numbering of the carbon atoms in the NMR spectra of the synthesized compounds is shown in Fig. 3. Mass spectra were carried out with a 6210 Time-of-Flight LC–MS instrument (G1969A, Agilent Technologies). The samples were dissolved in methanol in the presence of formic acid. A mobile phase stream (0.2% formic acid in water–methanol = 1:1) flow (0.2 mL/min) was introduced into the mass spectrometer using an Agilent Technologies 1200 Series HPLC instrument (Agilent Technologies,

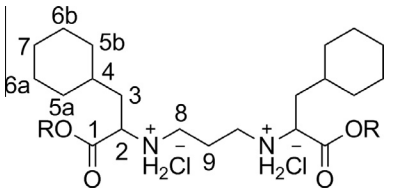

Fig. 3. The numbering of the carbon atoms in the NMR spectra of **1a–1e (R = H-1a, Me-1b, Et-1c, *n*Pr-1d, *n*Bu-1e)**.

Waldbronn, Germany) with binary pump, autosampler, column compartment (with ZDV cell instead of column) and DAD detector. Mass spectra were recorded in positive mode using the following conditions: capillary voltage 4000 V, gas temperature 350 °C, stream of the gas for drying 12 L/min, voltage fragmentor 140 V, mass range 100–3200 *m*/*z*.

Melting points were determined on an electrothermal melting point apparatus.

4.1.1. Synthesis of (S,S)-1,3-propanediamine-N,N′-di-2-(3-cyclohexyl) propanoic acid dihydrochloride, ***1a***

(*S*)-2-amino-3-cyclohexylpropanoic acid hydrochloride (1.00 g, 4.82 mmol) was slowly added to an ice-cooled solution of sodium hydroxide (10 mL, 1.25 M) and the solution was heated to 85 °C. Then, 1,3-dibromopropane (0.244 mL, 2.41 mmol) was added and the reaction mixture was refluxed for 24 h. The suspension was cooled to room temperature, filtered and the solid washed with a solution of sodium hydroxide (4 mL, 10 mM). The obtained acid was treated with a solution of HCl (20 mL, 1 M). The product was collected by filtration, washed with cold ethanol and dried under *vacuo*. Compound **1a** is a white powder. Yield: 0.52 g (47.4%); Mp: 248–250 °C; ^{1}H NMR (500.26 MHz, [D1]TFA): δ = 1.09 (m, C5a***H***, C5b***H***, 4H), 1.26–1.39 (m, C6a***H***, C6b***H***, 4H; C7***H***, 2H; N***H***, 1H), 1.66 (m, C4***H***, 2H), 1.76–1.92 (m, C5a′***H***, C5b′***H***, 4H; C6a′***H***, C6b′***H***, 4H; C7′***H***, 2H; N***H***, 1H), 2.05 (m, —C***H₂***Cy, 4H), 2.75 (m, —NH_2CH_2C***H₂***CH_2NH_2—, 2H), 3.58 and 3.63 (m, —NH_2C***H₂***CH_2C***H₂***-NH_2—, 4H), 4.35 (t, *J* = 7.0 Hz, HOOCC***H***—, 2H); ^{13}C NMR (125.79 MHz, [D1]TFA): 25.73 (—NH_2CH_2***C***$H_2CH_2NH_2$—), 27.40 (***C7***), 27.48 and 27.61 (***C6a*** and ***C6b***), 34.40 and 35.07 (***C5a*** and ***C5b***), 36.16 (***C4***), 39.59 (—***C***H_2Cy), 47.25(—NH_2***C***H_2CH_2***C***H_2NH_2—), 61.89 (HOOC***C***H—), 175.45 ppm (***C1***); IR (ATR): $\hat{\nu}$ = 3397.8, 2931.8, 2853.4, 2794.4, 1731.6, 1626.2, 1558.3, 1513.5, 1453.6, 1389.1, 1338.3, 1280.6, 1233.1, 1204.0, 1072.6, 813.4 cm^{-1}; ESI-MS: *m*/*z* (%): 383.29 (100) [M−2HCl+H]$^+$, 192.14 (73.09) [M−2HCl+2H]$^{2+}$; Anal. Calcd for $C_{21}H_{40}Cl_2N_2O_4$, %: C, 55.38; H, 8.85; N, 6.15. Found, %: C, 55.51; H, 9.13; N, 5.82.

4.1.2. Synthesis of O,O′-dimethyl-(S,S)-1,3-propanediamine-N,N′-di-2-(3-cyclohexyl)propanoate dihydrochloride, ***1b***

Thionyl chloride (4.5 mL) was added drop-wise into ice-cooled absolute methanol (30 mL) and then (*S*,*S*)-1,3-propanediamine-*N*,*N*′-di-2-(3-cyclohexyl)propanoic acid dihydrochloride (1.50 g, 3.30 mmol) was added. After stirring at 0 °C for 1 h, the suspension was refluxed for 24 h. The reaction mixture was filtered off and concentrated using a hot water-bath and, after addition of acetone, left at 4 °C The product was filtered, washed with methanol and dried under *vacuo*. Compound **1b** is a white powder. Yield: 0.84 g (52.8%); Mp: 200–202 °C; ^{1}H NMR (500.26 MHz, [D1]TFA): δ = 0.99 (m, C5a***H***, C5b***H***, 4H), 1.17–1.28 (m, C6a***H***, C6b***H***, 4H; C7***H***, 2H; N***H***, 1H), 1.46 (m, C4***H***, 2H), 1.69–1.80 (m, C5a′***H***, C5b′***H***, 4H; C6a′***H***, C6b′***H***, 4H; C7′***H***, 2H; N***H***, 1H), 1.93 (t, *J* = 7.0 Hz, —C***H₂***-Cy, 4H), 2.66 (m, —NH_2CH_2C***H₂***CH_2NH_2—, 2H), 3.44 and 3.53 (m, —NH_2C***H₂***CH_2C***H₂***NH_2—, 4H), 3.95 (s, C***H₃***OOC—, 6H), 4.23 (t, *J* = 7.0 Hz —OOCC***H***—, 2H); ^{1}H NMR (199.97 MHz, [D6]DMSO): δ = 0.87 (m, C5a***H***, C5b***H***, 4H), 1.08–1.25 (m, C6a***H***, C6b***H***, 4H; C7***H***, 2H), 1.46 (m, C4***H***, 2H), 1.59–1.87 (m, C5a′***H***, C5b′***H***, 4H; C6a′***H***, C6b′***H***, 4H; C7′***H***, 2H; —C***H₂***Cy, 4H), 2.15 (m, —NH_2CH_2C***H₂***-CH_2NH_2—, 2H), 2.95 and 3.04 (m, —NH_2C***H₂***CH_2C***H₂***NH_2—, 4H), 3.77 (s, C***H₃***OOC—, 6H), 4.00 (m, —OOCC***H***—, 2H); 9.61 and 10.04 (—CH_2N***H₂***$^+$—); ^{13}C NMR (125.79 MHz, [D1]TFA): 25.80 (—NH_2CH_2-***C***$H_2CH_2NH_2$—), 27.52 (***C7***), 27.57 and 27.67 (***C6a*** and ***C6b***), 34.44 and 35.17 (***C5a*** and ***C5b***), 36.27 (***C4***), 39.65 (—***C***H_2Cy), 47.28 (—NH_2-***C***H_2CH_2***C***H_2NH_2—), 56.12 (***C***H_3OOC—), 62.33 (—OOC***C***H—), 173.22 ppm (***C1***); IR (ATR): $\hat{\nu}$ = 2929.2, 2854.7, 2712.3, 2649.2, 2452.0, 1741.8, 1528.9, 1475.0, 1453.2, 1336.5, 1282.3, 1241.2, 1207.4, 1078.6, 841.9 cm^{-1}; ESI-MS: *m*/*z* (%): 411.32 (100) [M−2HCl+H]$^+$, 206.16 (51.05) [M−2HCl+2H]$^{2+}$; Anal. Calcd for C_{23}-$H_{44}Cl_2N_2O_4$, %: C, 57.13; H, 9.17; N, 5.79. Found, %: C, 57.05; H, 9.44; N, 6.02.

4.1.3. Synthesis of O,O′-diethyl-(S,S)-1,3-propanediamine-N,N′-di-2-(3-cyclohexyl)propanoate dihydrochloride, ***1c***

O,*O*′-diethyl-(*S*,*S*)-1,3-propanediamine-*N*,*N*′-di-2-(3-cyclohexyl) propanoate dihydrochloride was prepared as described above using absolute EtOH. Compound **1c** is a white powder. Yield: 0.94 g (55.9%); Mp: 204–206 °C; ^{1}H NMR (500.26 MHz, [D1]TFA): δ = 0.98 (m, C5a***H***, C5b***H***, 4H), 1.17–1.26 (m, C6a***H***, C6b***H***, 4H; C7***H***, 2H; N***H***, 1H), 1.37 (t, *J* = 7.5 Hz, C***H₃***CH_2OOC—, 6H), 1.49 (m, C4***H***, 2H), 1.70–1.83 (m, C5a′***H***, C5b′***H***, 4H; C6a′***H***, C6b′***H***, 4H; C7′***H***, 2H; N***H***, 1H), 1.92 (t, *J* = 7.0 Hz, —C***H₂***Cy, 4H), 2.64 (m, —NH_2-CH_2C***H₂***CH_2NH_2—, 2H), 3.43 and 3.54 (m, —NH_2C***H₂***CH_2C***H₂***NH_2—, 4H), 4.21 (t, *J* = 7.0 Hz, —OOCC***H***—, 2H), 4.38 and 4.45 (m, CH_3C***H₂***-OOC—, 4H); ^{13}C NMR (125.79 MHz, [D1]TFA): 14.47 (***C***H_3CH_2-OOC—), 25.72 (—NH_2CH_2***C***$H_2CH_2NH_2$—), 27.44 (***C7***), 27.55 and 27.58 (***C6a*** and ***C6b***), 34.27 and 35.19 (***C5a*** and ***C5b***), 36.31 (***C4***), 39.66 (—***C***H_2Cy), 47.17 (—NH_2***C***H_2CH_2***C***H_2NH_2—), 62.36 (—OOC***C***H—), 67.20 (CH_3***C***H_2OOC—), 172.77 ppm (***C1***); IR (ATR): $\hat{\nu}$ = 3435.1, 2928.4, 2854.1, 2721.8, 2455.3, 1739.1, 1550.5, 1455.5, 1372.4, 1279.4, 1235.5, 1197.8, 1039.1, 1008.9, 852.4 cm^{-1}; ESI-MS: *m*/*z* (%): 439.35 (100) [M−2HCl+H]$^+$, 220.17 (63.59) [M−2HCl+2H]$^{2+}$; Anal. Calcd for $C_{25}H_{48}Cl_2N_2O_4$, %: C, 58.70; H, 9.46; N, 5.48. Found, %: C, 58.35; H, 9.20; N, 5.33.

4.1.4. Synthesis of O,O′-di-n-propyl-(S,S)-1,3-propanediamine-N,N′-di-2-(3-cyclohexyl)propanoate dihydrochloride, ***1d***

O,*O*′-dipropyl-(*S*,*S*)-1,3-propanediamine-*N*,*N*′-di-2-(3-cyclohexyl)propanoate dihydrochloride was prepared as described above using absolute *n*-PrOH. Compound **1d** is a white powder. Yield: 0.96 g (53.9%); Mp: 198–200 °C; ^{1}H NMR (500.26 MHz, [D1]TFA): δ = 1.14 (m, C5a***H***, C5b***H***, 4H; C***H₃***CH_2CH_2OOC—, 6H), 1.31–1.41 (m, C6a***H***, C6b***H***, 4H; C7***H***, 2H; N***H***, 1H), 1.64 (m, C4***H***, 2H), 1.83–1.98 (m, C5a′***H***, C5b′***H***, 4H; C6a′***H***, C6b′***H***, 4H; C7′***H***, 2H; N***H***, 1H, CH_3C***H₂***CH_2OOC—, 4H), 2.06 (t, *J* = 7.0 Hz, —C***H₂***Cy, 4H), 2.78 (m, —NH_2CH_2C***H₂***CH_2NH_2—, 2H), 3.57 and 3.68 (m, —NH_2C***H₂***-CH_2C***H₂***NH_2—, 4H), 4.36 (t, *J* = 7.0 Hz, —OOCC***H***—, 2H), 4.42 and 4.49 (m, CH_3CH_2C***H₂***OOC—, 4H); ^{13}C NMR (125.79 MHz, [D1]TFA): 10.86 (***C***$H_3CH_2CH_2$OOC—), 23.47 (CH_3***C***H_2CH_2OOC—), 25.82 (—NH_2-CH_2***C***$H_2CH_2NH_2$—), 27.52 (***C7***), 27.64 and 27.66 (***C6a*** and ***C6b***), 34.31 and 35.32 (***C5a*** and ***C5b***), 36.38 (***C4***), 39.81 (—***C***H_2Cy), 47.22 (—NH_2***C***H_2CH_2***C***H_2NH_2—), 62.43 (—OOC***C***H—), 72.81 (CH_3-CH_2***C***H_2OOC—), 173.00 ppm (***C1***); IR (ATR): $\hat{\nu}$ = 3447.0, 2927.5, 2855.7, 2721.8, 2551.3, 2454.5, 1737.4, 1551.8, 1458.5, 1396.1, 1279.8, 1234.8, 1198.1, 1055.8, 925.9 cm^{-1}; ESI-MS: *m*/*z* (%): 467.38 (100) [M−2HCl+H]$^+$, 234.19 (71.83) [M−2HCl+2H]$^{2+}$; Anal. Calcd for $C_{27}H_{52}O_4N_2Cl_2$, %: C, 60.10; H, 9.71; N, 5.19. Found, %: C, 60.42; H, 10.00; N, 4.88.

4.1.5. Synthesis of O,O′-dibutyl-(S,S)-1,3-propanediamine-N,N′-di-2-(3-cyclohexyl)propanoate dihydrochloride, ***1e***

O,*O*′-di-*n*-butyl-(*S*,*S*)-1,3-propanediamine-*N*,*N*′-di-2-(3-cyclohexyl)propanoate dihydrochloride was prepared as described

above using absolute *n*-BuOH. Compound **1e** is a white powder. Yield: 1.11 g (59.4%); Mp: 200 °C; ^{1}H NMR (500.26 MHz, [D1]TFA): δ = 0.96 (t, J = 7.5 Hz, C***H*****$_3$**CH$_2$CH$_2$CH$_2$OOC—, 6H), 1.05 (m, C5a***H***, C5b***H***, 4H), 1.19–1.29 (m, C6a***H***, C6b***H***, 4H; C7***H***, 2H; N***H***, 1H), 1.47 (m, C4***H***, 2H; CH$_3$C***H*****$_2$**CH$_2$CH$_2$OOC—, 4H), 1.73–1.86 (m, C5a′***H***, C5b′***H***, 4H; C6a′***H***, C6b′***H***, 4H; C7′***H***, 2H; N***H***, 1H; CH$_3$CH$_2$-C***H*****$_2$**CH$_2$OOC—, 4H), 1.94 (t, J = 6.0 Hz, —C***H*****$_2$**Cy, 4H), 2.66 (m, —NH$_2$-CH$_2$C***H*****$_2$**CH$_2$NH$_2$—, 2H), 3.46 and 3.56 (m, —NH$_2$C***H*****$_2$**CH$_2$C***H*****$_2$**NH$_2$—, 4H), 4.24 (m, —OOCC***H***—, 2H), 4.36 and 4.42 (m, CH$_3$CH$_2$CH$_2$C***H*****$_2$**-OOC—, 4H); ^{13}C NMR (125.79 MHz, [D1]TFA): 14.12 (***C***H$_3$CH$_2$CH$_2$-CH$_2$OOC—), 20.83 (CH$_3$***C***H$_2$CH$_2$CH$_2$OOC—), 25.84 (—NH$_2$CH$_2$***C***H$_2$CH$_2$NH$_2$—), 27.54 (***C7***), 27.68 (***C6a*** and ***C6b***), 32.20 (CH$_3$CH$_2$***C***H$_2$CH$_2$OOC—), 34.32 and 35.38 (***C5a*** and ***C5b***), 36.41 (***C4***), 39.81 (—***C***H$_2$Cy), 47.25 (—NH$_2$***C***H$_2$CH$_2$***C***H$_2$NH$_2$—), 62.46 (—OOC***C***H—), 71.12 (CH$_3$CH$_2$CH$_2$***C***H$_2$OOC—), 172.99 ppm (***C1***); IR (ATR): $\hat{\nu}$ = 3451.0, 2930.1, 2856.1, 2722.5, 2456.5, 1742.5, 1549.9, 1470.6, 1361.8, 1278.5, 1235.4, 1196.4, 1064.2 cm^{-1}; ESI-MS: m/z (%): 495.41 (100) [M−2HCl+H]$^+$, 248.20 (69.62) [M−2HCl+2H]$^{2+}$; Anal. Calcd for $C_{29}H_{56}O_4N_2Cl_2$, %: C, 61.36; H, 9.94; N, 4.93. Found, %: C, 61.12; H, 9.95; N, 5.05.

4.2. Biology

4.2.1. Cell cultures and reagents

Reagents used in the biological experiments were obtained from Sigma (St. Louis, MO, USA) unless stated otherwise. The human neuroblastoma (SH-SY5Y), human promyelocytic leukaemia (HL-60), human (U251) and rat (C6) glioma and mouse fibrosarcoma (L929) cell lines were obtained from European Collection of Cell Cultures (ECACC; Salisbury, UK). Primary astrocyte cultures were established from brains of newborn Wistar rats according to the method developed by McCarthy and De Vellis [26]. Cell cultures were maintained at 37 °C in a humidified atmosphere with 5% CO_2, in HEPES-buffered (20 mM) RPMI 1640 cell culture medium supplemented with 5% foetal calf serum, 2 mM L-glutamine, 10 mM sodium pyruvate, penicillin/streptomycin mixture (all from PAA, Pasching, Austria) and 6 g/L glucose for primary astrocytes. The cells were prepared for experiments by using the conventional trypsinization procedure with trypsin/EDTA and incubated in 96-well flat-bottom plates (1×10^4 cells per well except astrocytes: 4×10^4 cells per well) for cell viability assessment or in 6-well plates (3×10^5 cells per well except astrocytes: 6×10^5 cells) for flow cytometric analysis. The cultures of Wistar rat primary astrocytes were conducted on 21-day-old astrocyte cultures that were trypsinized at least twice, and the cells' maturity was verified using GFAP-FITC immunostaining (Fig. 3A). Cells were allowed to rest for 24 h and than treated with novel compounds **1a**–**1e** previously dissolved in formic acid (**1a**) or ethanol (**1b**–**1e**) according to their solubility and kept at room temperature until use. In each experiment, an additional control cell culture contained the appropriate amount (the maximum that was used) of the corresponding solvent. The results showed no difference in comparison with the results for the untreated cells and so the results are presented only for untreated cells as the control. Formic acid was only toxic to the primary rat astrocyte cell culture and therefore the IC_{50} value for parental acid **1a** on astrocytes was not calculated.

4.2.2. Cytotoxic assays

The MTT assay [3-(4,5-dimethylthiazol-2-yl)-2,5-diphenyl tetrazolium bromide], which determines the mitochondrial dehydrogenase activity, and the lactate dehydrogenase (LDH) assay, which is a marker of cell membrane damage, were used to measure cell viability. The tests were performed as previously described [22] and the results are presented as % of the control viability (MTT) arbitrarily set to 100% and as % cytotoxicity (LDH) using Tryton X-100-lysed untreated cells as a positive control. The IC_{50} values for the investigated compounds were determined using GraphPad Prism.

4.2.3. Flow cytometry assessment of apoptosis, oxidative stress and autophagy

Flow cytometry analysis was performed on a FACSCalibur flow cytometer (BD Biosciences, Heidelberg, Germany) using CellQuest Pro software for acquisition and analysis. The light-scatter channels were set on linear gains and the fluorescence channels on a logarithmic scale. A minimum of 10,000 cells was analyzed in each condition, adjusting the threshold settings so that the cell debris was excluded from the data acquisition. The size and density of cells were assessed using forward scatter (FSC) and side scatter (SSC), respectively.

4.2.3.1. Apoptosis assessment. The type of cell death (apoptotic or necrotic) was analyzed by double staining with annexin-V-fluorescein isothiocyanate (FITC), which binds to early apoptotic cells with exposed phosphatidylserine, and propidium iodide (PI), which labels the late apoptotic/necrotic cells with membrane damage (staining kit from BD Pharmingen, San Diego, CA). Activation of caspases was assessed by measuring the increase in the green fluorescence (FL1) of a cell-permeable FITC-conjugated pan-caspase inhibitor (ApoStat; R&D Systems, Minneapolis, MN) according to the manufacturer's instructions. The increase in green fluorescence (FL1) was considered as a measure of caspase activity.

4.2.3.2. Cell cycle analysis. The cell cycle was analyzed and DNA fragmentation determined by flow cytometric quantification of nuclear DNA of ethanol-fixed cells stained with DNA-binding dye (red fluorescence, FL2 channel) PI as previously described [22]. The hypodiploid cells (sub-G0 compartment) were considered apoptotic.

4.2.3.3. Oxidative stress and reactive oxygen species production. The total intracellular production of reactive oxygen species (ROS) was determined by measuring the intensity of green fluorescence emitted by a non-selective redox-sensitive dye dihydrorhodamine 123 (DHR; Invitrogen, Paisley, UK), which was added to cell cultures (5 μM) at the beginning of treatment. At the end of incubation, cells were detached by trypsinization, washed in PBS and the increase in green fluorescence (FL1) was analyzed as a measure of ROS production. The mitochondrial production of superoxide was analyzed using flow cytometry by measuring the intensity of red fluorescence (FL2) emitted by a superoxide-specific fluorochrome, dihydroethidium (DHE; Sigma–Aldrich), which was incubated with cells (20 μM) for 30 min at the end of the treatment.

4.2.3.4. Autophagy assessment. Acidic autophagolysosomes were detected by flow cytometric analysis of the cells stained with a pH-sensitive supravital dye (acridine orange) that stains cytoplasmic autophagolysosomes orange-red and nuclei green. Therefore, autophagy is detected as an increase in the red/green fluorescence ratio (FL3/FL1). After incubation, cells were washed with PBS and stained with acridine orange (1 μM) for 15 min at 37 °C. Cells were than trypsinized, washed in PBS and analyzed on a flow cytometer.

4.2.4. Statistical analysis

The statistical significance of the differences was analyzed using the Student t-test for small independent samples. A value of $p < 0.05$ was considered significant.

Acknowledgments

This work was supported by the Ministry of Education, Science and Technological development of the Republic of Serbia, Grant Numbers 172035, 41025 and Innovative Project Number 451-03-2372-IP.

Appendix A. Supplementary material

Supplementary data associated with this article can be found, in the online version, at http://dx.doi.org/10.1016/j.bioorg.2014.04.006.

References

[1] S. Laufer, U. Holzgrabe, D. Steinhilber, Angew. Chem. 52 (2013) 4072–4076.
[2] C. Avendaño, J.C. Menédez, Medicinal Chemistry in Anticancer Drugs, first ed., Elsevier, Amsterdam, 2008.
[3] E. Alessio, Bioinorganic Medicinal Chemistry, first ed., Wiley-VCH, Weinheim, 2011.
[4] I. Kostova, Recent Pat. Anti-Cancer 1 (2006) 1–22.
[5] N.J. Wheate, S. Walker, G.E. Craig, R. Oun, Dalton Trans. 39 (2010) 8113–8127.
[6] A.G. Quiroga, J. Inorg. Biochem. 114 (2012) 106–112.
[7] M. Galanski, M.J. Jakupec, B.K. Keppler, Curr. Med. Chem. 18 (2005) 2075–2094.
[8] A. Bergamo, G. Sava, Dalton Trans. 40 (2011) 7817–7823.
[9] W.H. Ang, A. Casini, G. Sava, P.J. Dyson, J. Organomet. Chem. 696 (2011) 989–998.
[10] R. Gogna, E. Madan, B.K. Keppler, U. Pati, Brit. J. Pharmacol. 166 (2012) 617–636.
[11] N.M. Martins, N.A. Santos, C. Curti, M.L. Bianchi, A.C. Santos, J. Appl. Toxicol. 28 (2008) 337–344.
[12] E. Estrada, E. Uriarte, A. Montero, M. Teijeira, L. Santana, E.J. De Clercq, Med. Chem. 43 (2000) 1975–1985.
[13] A.R. Timerbaev, C.G. Hartinger, S.S. Aleksenko, B.K. Keppler, Chem. Rev. 106 (2006) 2224–2248.
[14] K.S. Lovejoy, S.J. Lippard, Dalton Trans. (2009) 10651–10659.
[15] L.E. Mihajlović, A. Savić, J. Poljarević, I. Vučković, M. Mojić, M. Bulatović, D. Maksimović-Ivanić, S. Mijatović, G.N. Kaluđerović, S. Stošić-Grujičić, Đ. Miljković, S. Grgurić-Šipka, T.J. Sabo, J. Inorg. Biochem. 109 (2012) 40–48.
[16] G.N. Kaluđerović, H. Schmidt, S. Schwieger, C. Wagner, R. Paschke, A. Dietrich, T. Mueller, D. Steinborn, Inorg. Chim. Acta 361 (2008) 1395–1404.
[17] J.M. Vujić, G.N. Kaluđerović, M. Milovanović, B.B. Zmekovski, V. Volarević, D. Živić, P. Đurđević, N. Arsenijević, S.R. Trifunović, Eur. J. Med. Chem. 46 (2011) 4559–4565.
[18] J.M. Lazić, Lj. Vučićević, S. Grgurić-Šipka, K. Janjetović, G.N. Kaludjerović, M. Misirkić, M. Gruden-Pavlović, D. Popadić, R. Paschke, V. Trajković, T.J. Sabo, ChemMedChem 5 (2010) 881–889.
[19] S. Misirlic Dencic, J. Poljarevic, U. Vilimanovich, A. Bogdanovic, A.J. Isakovic, T. Kravic Stevovic, M. Dulovic, N. Zogovic, A.M. Isakovic, S. Grguric-Sipka, V. Bumbasirevic, T.J. Sabo, V. Trajkovic, I. Markovic, Chem. Res. Toxicol. 25 (2012) 931–939.
[20] J. Wang, Y. Chen, J. Ren, C. Zhao, X. Qu, Nucl. Acids Res. 42 (2014) 3792–3802.
[21] The Intellectual Property Office of the Republic Serbia, Patent Application No. P-2013/0270, June 28, 2013.
[22] N. Raicević, A. Mladenović, M. Perović, L. Harhaji, D. Miljković, V. Trajković, Neuropharmacology 48 (2005) 720–731.
[23] M.C. Maiuri, E. Zalckvar, A. Kimchi, G. Kroemer, Nat. Rev. Mol. Cell Biol. 8 (2007) 741–752.
[24] S. Riedl, Y. Shi, Nat. Rev. Mol. Cell Biol. 5 (2004) 897–907.
[25] L. Harhaji, A. Isakovic, N. Raicevic, Z. Markovic, B. Todorovic-Markovic, N. Nikolic, S. Vranjes-Djuric, I. Markovic, V. Trajkovic, Eur. J. Pharmacol. 568 (2007) 89–98.
[26] K.D. McCarthy, J. De Vellis, J. Cell Biol. 85 (1980) 890–902.